

# Metrology for Phase-Referenced Imaging and Narrow-Angle Astrometry with the VLTI

Samuel Lévêque  
European Southern Observatory  
Karl Schwarzschild Str.2, D-85748 Garching bei München  
[sleveque@eso.org](mailto:sleveque@eso.org)

## ABSTRACT

The capability to perform Phased-Reference Imaging and Narrow-Angle Astrometry with the VLTI will be given by the PRIMA instrument, which is based on the simultaneous observation of two celestial objects. A highly accurate metrology system is required to monitor the optical path followed by the two objects inside the VLTI. In the framework of PRIMA, this paper reviews the requirements as well as the constraints for such a metrology system and discusses its implementation.

**Keywords:** Laser metrology, Interferometry, VLTI

## 1. INTRODUCTION

The “Phase-Referenced Imaging and Micro-arcsecond Astrometry” (PRIMA) facility<sup>1</sup> of the VLTI is based on the simultaneous coherent observation of two celestial objects in which the two interferometric signals are tied together by an internal metrology system. The role of this metrology system is to monitor the PRIMA instrumental optical path errors to possibly reach a final instrumental phase accuracy limited by atmospheric piston anisoplanatism<sup>2</sup>.

In order to place the metrology system in the context of PRIMA, let us consider two celestial objects of vector coordinates  $S_1$  and  $S_2$ , simultaneously observed on two independent beam combiners, i.e. using a dual-feed configuration. By stabilizing the interference fringes on the so-called reference object  $S_1$ , the residual Optical Path Difference,  $\Delta\text{OPD}$ , seen by  $S_2$  is given by:

$$\Delta\text{OPD} = B \cdot (S_2 - S_1) + \phi/k + \delta A + \Delta L \quad \text{Eq.(1)}$$

- $B$  is the vector baseline of the interferometer
- $\phi$  is a phase factor inherent to the nature of the observed objects and is the observable for phased-referenced imaging,  $k$  being the wave number.
- $\delta A$  represents the OPD (or piston) anisoplanatism which contributes to the residual fringe motion seen by  $S_2$ . For the maximum angular separation  $S_2 - S_1$  of PRIMA of 1 arcmin, the standard deviation of  $\delta A$  is about 10 times lower than the open-loop atmospheric fringe motion imposed on  $S_1$ .  $\delta A$  has a zero mean and can be averaged-out by successive measurements of  $\Delta\text{OPD}$  in a typical 30 min. time frame for a 10 arcsec star separation and a  $10\mu\text{arcsec}$  astrometric accuracy.
- $\Delta L = L_2 - L_1$  represents the difference between the internal OPD's of each object.  $\Delta L$  can thus be seen as the instrumental contribution to  $\Delta\text{OPD}$ .

Knowing the baseline vector  $B$  and by measuring independently  $\Delta\text{OPD}$  and  $\Delta L$ , Eq.(1) shows that one can estimate either the factor  $\phi$  for a known star separation (Phase-referenced Imaging mode), or inversely the star separation for a known  $\phi$  (Astrometric mode). The bottom line being that the implementation of PRIMA is intimately linked with the ability to trace back the "differential" internal OPD between the two objects,  $\Delta L$ .

The following sections will detail the requirements of such a metrology system, analyze the constraints and finally discuss its implementation.

## 2. THE REQUIREMENTS AND THE CONSTRAINTS

In observing conditions, the amplitude of  $\Delta L$  can reach about 60 mm. This corresponds to  $\Delta OPD$  obtained for a maximum star separation  $S_2-S_1$  of 1 arcmin and a 200 m projected baseline. In the PRIMA configuration, both celestial objects' beams share the same Delay Lines, which consequently act on  $L_1$  and  $L_2$  in a similar way. Therefore,  $\Delta L$  is not modified by the displacement of the Delay Lines but is only affected, in a first order, by the motion of the Differential Delay Lines, which act only on  $L_2$ .

Given the above internal geometry, simply monitoring the OPD created by the Differential Delay Lines would be in principle sufficient to determine  $\Delta L$ . However, this statement is only true for an infinitely stable interferometer, i.e. where no internal OPD de-correlates the fringe positions of  $S_1$  and  $S_2$ . In reality, such an OPD will occur due to, for example, internal air turbulence or optics imperfection. From a metrology point of view, this OPD can be compared to a dead path error occurring in a distance measuring laser interferometer. We measured, inside the delay line tunnel at Parana<sup>3</sup>, the optical path fluctuations between two parallel beams separated by 240 mm, i.e. according to the PRIMA beam geometry. The results showed that the standard deviation of these fluctuations can reach about 1  $\mu\text{m}$  during a 10 min observation and for a 80 m propagation length. These fluctuations are already above the accuracy requirement set on  $\Delta L$  as shown here below. Therefore, the metrology system must monitor the entire internal path of the VLTI, i.e. along few hundred meters, to obtain an accurate estimation of  $\Delta L$ . However, the amplitude of  $\Delta L$  will remain typically in the 60 mm range.

The accuracy requirement on  $\Delta L$  is driven by the astrometric mode but it can be relaxed by a factor 50 to 100 in the imaging mode, and depending on the observing parameters. For an astrometric accuracy goal of  $\theta=10\mu\text{arcsec}$ , and a baseline of  $B=100\text{m}$ ,  $\Delta L$  must be known with a  $B\cdot\theta=5\text{nm}$  accuracy or  $\lambda/200$  for  $\lambda=1\ \mu\text{m}$ . It is important to recall that this astrometric accuracy also assumes an object separation of 10 arcsec and a 30 min observation to average out the OPD anisoplanatism<sup>4</sup>. Therefore, any quasi-stationary random errors on  $\Delta L$ , with a zero mean over 30 min, will also be averaged out. On the other hand, care must be taken to minimize any drift of the metrology within this time scale.

In the astrometric mode, a fringe phase measurement on the secondary channel will typically occur every  $T_{\text{exp}}=55\text{msec}$  (respectively 40 msec) to freeze any anisoplanatism effects for objects separated by 10 arcsec (respectively 1 arcmin). These exposure times correspond to a tolerated 10% visibility loss at  $\lambda=2.2\ \mu\text{m}$ , or equivalently to residual OPD error of  $\lambda/14$ . Therefore,  $T_{\text{exp}}$  can also be used to average out some high frequency metrology errors.

In addition to an ambitious accuracy goal, the metrology system has to cope with several constraints. Among them:

- It has to deal with long propagation paths. As an example, the distance between the Auxiliary Telescope (AT) J6 station and the interferometric laboratory, going through the underground light ducts and tunnel, can reach some 276m, including a maximum 120 m distance introduced by the delay line.
- The beams are relayed through air as opposed to vacuum, thus undergoing both slight OPD fluctuations and beam wander due to internal turbulence. Details about the amplitude of these phenomena can be found in <sup>3</sup>.
- To possibly reach the astrometric accuracy goal, the metrology system and the stellar beams must share the same internal path, and in particular share the beam combiners where the stellar fringes are formed. Otherwise any "non-common" path variations must be maintained at the nm level. For a laser based metrology system, this implies that modifying specific characteristics of the laser beam, after it is injected in the stellar path, similarly affects the stellar light. This pertains in particular to (i) OPD modulation and in some cases to (ii) the injection/separation of polarization-encoded heterodyne components of the laser beam. Both schemes being commonly used in laser metrology systems.
- Sharing the light path also impose a careful management of the interfaces with all VLTI sub-systems (e.g. delay lines, telescope optics,...), including possible straylight contamination on existing detectors (e.g. field stabilization sensor, wavefront sensor, instrument's detector). This limits both the wavelength and power allocation for a laser metrology system. The metrology is the only PRIMA sub-system having interfaces with all other PRIMA sub-systems.

### 3. IMPLEMENTATION BASELINE FOR THE METROLOGY SYSTEM

Driven by the above accuracy requirements, constraints, and metrology state of the art, the PRIMA metrology system shall be based on heterodyne laser interferometry. This technique has clear advantages in terms of sensitivity as well as immunity to noise and cross-talk. Because such a system is purely incremental (i.e. counting the number of  $2\pi$  phase variation while  $\Delta L$  is evolving), the estimation of the *absolute* value of  $\Delta L$  implies an accurate calibration the metrology "zero" point ( $\Delta L=0$ ). The current scheme for this calibration consists in the simultaneous observation of the reference celestial object on both PRIMA channels<sup>1</sup>. White light interferometry using an internal source (i.e no stellar light anymore) is currently under investigation<sup>6</sup>.

The implementation of an absolute metrology system<sup>7</sup> for PRIMA is clearly more ambitious than an incremental one since all problems related to incremental metrology, which are sharp already, must be previously tackled. Nevertheless, it remains a potential solution to overtake the current calibration scheme and thus reducing the complexity of the star separator<sup>1</sup>. In this case, the complexity of the PRIMA star separator is simply transferred to the metrology system.

An implementation baseline for the metrology system has been identified during the PRIMA feasibility study<sup>5</sup>, based on a trade-off analysis. It consists in a telescope pair-wise configuration: the internal optical path difference is monitored for each celestial object from its beam combiner to reference points located in both telescopes. Therefore, it involves two similar heterodyne laser interferometers and  $\Delta L$  is obtained by monitoring the difference between the 2 interferometers. For each interferometer, the propagation path to the reference points and back can reach up to  $2 \times 276 = 552$  m (return way) with the J6 AT's station J6 and 472 m with the UT's, the OPD introduced by the Delay Lines being about  $2 \times 120 = 240$  m .

The main sub-systems of the metrology and their characteristics are presented below:

- **Laser head**

Considering that only  $\Delta L$  is relevant and that  $\Delta L$  is less than about 60mm, a single laser head will be used for both metrology systems to possibly relax the wavelength stability requirements. The stability limit is given by  $5\text{nm}/60\text{mm} \sim 8.10^{-8}$  instead of  $5\text{nm}/240\text{m} \sim 2.10^{-11}$ . However, the coherence length of the laser (i.e. its linewidth) must still be compatible with an OPD of 240m. Additional power and wavelength compatibility considerations led to the selection of a Nd-YAG laser emitting at a wavelength of 1064 nm.

- **Heterodyne assembly**

In order to minimize cross-talk perturbations, the laser interferometers will operate at two different heterodyne frequencies,  $f_1$  and  $f_2$ , separated by  $\Delta\nu$  and generated from the laser frequency  $\nu$ , as shown in Figure 1. These frequencies are traditionally generated using acousto-optics modulators.

The selection of the bandwidth around each heterodyne frequency depends on the dynamic requirements set on the individual interferometer. In the baseline configuration, a dynamic phase variation in the  $\delta f = 25$  kHz range (at  $\lambda = 1\mu\text{m}$ ) will be imposed on both interferometers. This number comes from the necessity to follow the internal OPD created by the delay lines in the tracking mode, including the atmospheric compensation. For the interferometer, which includes the path of the Differential Delay Lines, an additional phase variation of about 10 Hz will occur in the tracking mode, thus negligible w.r.t the above 25 kHz. In order to operate this interferometer while slewing the DDL, e.g. during calibration, its bandwidth must be extended by typically 10 kHz. This number corresponds to covering an OPD of  $2 \times 60\text{mm}$  (return path) with the DDL in 12 sec.

The heterodyne frequencies should be high enough to accommodate the required bandpass,  $\delta f$ , in a frequency region well above the intensity noise, including amplitude fluctuations of the laser head. The upper value of the heterodyne frequency is primarily imposed by the resolution of the metrology for a fixed clock frequency (see phase meter section).  $\Delta\nu$  allows to reject any cross-talk noise well outside the heterodyne frequency bands and outside the DC- $f_2$  region.

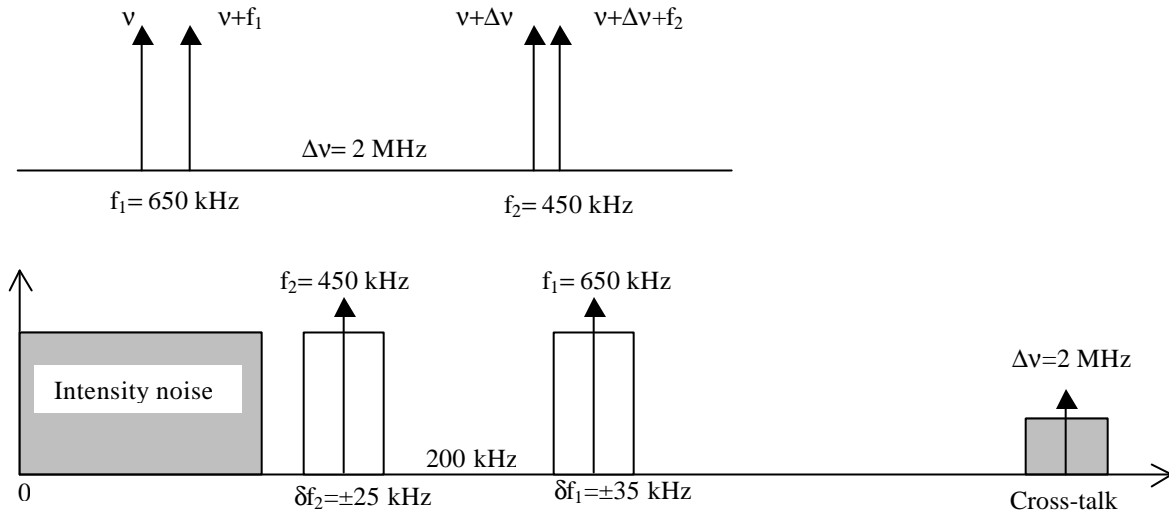


**Figure 1: Possible Metrology frequency allocation**

- **Phase meter**

A heterodyne interferometer generates a reference signal and a probe signal, each beating at the heterodyne frequency,  $f$ . The optical path difference information is coded in the phase difference,  $\phi$ , between these two signals. The performance of the PRIMA metrology system critically depends on the ability to accurately demodulate the phase.

The concept for the PRIMA phase detection has been studied recently<sup>6</sup>. As shown in Figure 2, the principle consists in first electronically mixing the two interferometer signals followed bandpass filtering around the "super-heterodyne frequency"  $f_1 - f_2 = 200\text{kHz}$ . In this way, one obtains directly the relevant information about  $\Delta L$ . Thus, there is no need to compute  $\Delta L$  from the difference between the individual phase measurements  $\phi_1$  and  $\phi_2$  delivered by the two interferometers, which would require an accurate synchronization.

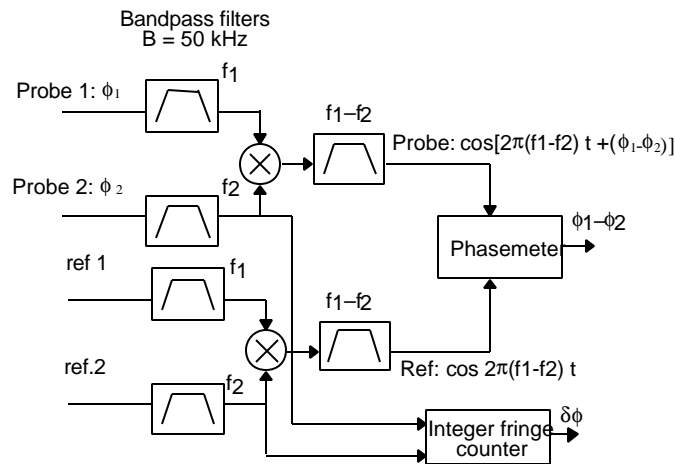


**Figure 2: Super-heterodyne phase detection<sup>6</sup>**

Phase demodulation techniques can be divided into two main types:

- Synchronous demodulation type, which involves signal multiplication and low pass filtering
- "Trigger" based techniques including amplitude or time interval measurements

With nowadays availability of always faster clocks, trigger techniques are increasingly applied and can be found in commercial systems such as in the ZMI-1000 interferometer from Zygo Corp. The calibration constraints are greatly reduced as well as the sensitivity to electronics drifts. A trade-off analysis<sup>6</sup> has shown that a digital zero-crossing phase meter is the most promising demodulation scheme for the PRIMA metrology. The principle consists in measuring the number of clock periods between the leading edge of the reference signal and of the probe signal. A block diagram of possible phase meter architecture is shown in Figure 3. The resolution is proportional to the ratio between the super-heterodyne frequency and the clock frequency. Given a 200kHz super-heterodyne frequency, the clock must operate at 200MHz for a  $2\pi/1000$  resolution. The time base signal is directly generated from the reference signal using a Phase-Locked Loop, thus minimizing any phase drift errors (no calibration needed). Another way would be to generate all frequencies driving the acousto-optics modulators (and thus generating all the heterodyne frequencies) from a given time base signal. However, but this would require a significantly higher clock frequency.

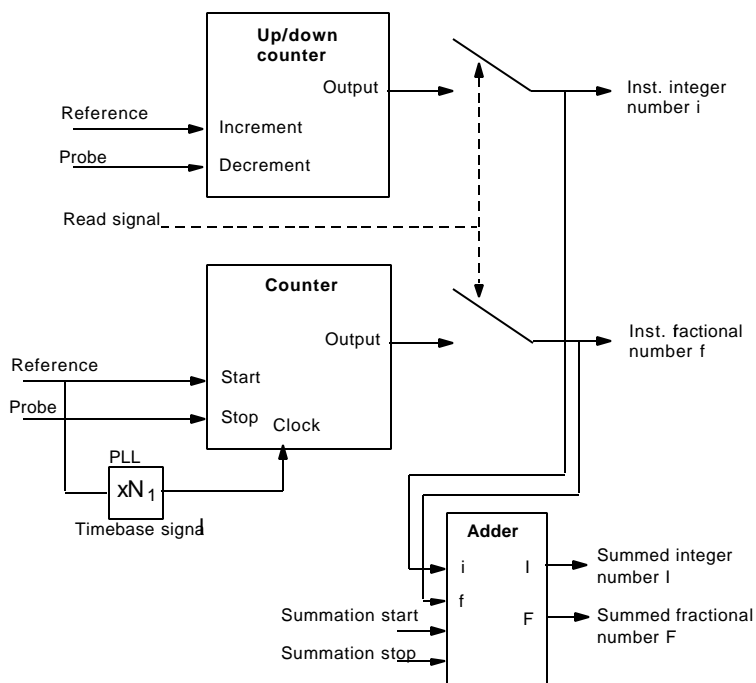


**Figure 3: Phase meter block diagram<sup>6</sup>**

- **Metrology beam injection**

In order to minimize the non-common path between the laser and the stellar beams, the separation and re-combination of the metrology beam should be performed directly by the stellar beam combiner. By forming an image of the telescope's pupil on this beam combiner, a possible approach consists in injecting/combining the metrology beam inside the central obscuration. However, this configuration requires that the frequency shifted heterodyne components of the metrology be spatially super-imposed, i.e the implementation of a polarization heterodyne scheme. Thus, a polarization beam splitter must be located in the pupil central obscuration to separate the frequency shifted p and s polarization state of the laser beam.

For a pupil image of 80mm diameter located in the interferometric laboratory, the diameter of the central obscuration is about 11mm. Considering the large distances involved and the number of optical surfaces, the effect of both diffraction and rotation of the polarization state must be quantified.

In order to assess the feasibility of this approach in the context of the VLTI, the propagation of the laser beam along the VLTI optical train was simulated using an algorithm based on Gaussian beam superposition. This algorithm has been recently implemented<sup>8</sup> into the ESO end-to-end model of the VLTI. A Gaussian beam was injected from a pupil plane (u-w coordinates) located in the interferometric laboratory with the following characteristics:

- Mode: Gaussian, TEM<sub>00</sub>
- Polarization: Linear (w-direction)

- Wavelength:  $\lambda=1 \mu\text{m}$
- Power: 1 mW
- Waist size: 4.1 mm, thus fitting in the central obscuration of the starlight beam

In order to fully model diffraction effects, the injected Gaussian beam was first decomposed into a set of 421 fundamental Gaussian beams, each having a waist radius of 0.5 mm. The full set of fundamental beams propagated up to the retro-reflector, using a "beam tracing method", where the incoming electric vector field was computed by superposing the contribution of each fundamental beam. A "perfect" retro-reflector was located in an image of the telescope's central obscuration at the center of the secondary mirror (see next section ). The simulation was conducted for the VLTI Unit Telescope. The total propagation distance was about 177 m, i.e. about 2.6 times the Rayleigh length of the injected beam. The retro-reflector had a diameter limited to 120 mm to possibly fit within the image of the central obscuration. At this point, a second decomposition was necessary to simulate the effect of beam clipping, as shown in Figure 4.

Propagation back to the "injection" pupil plane in the interferometric laboratory yielded the beam profile of the returning beam shown in Figure 5. The polarization mode of the returning beam, shown in Figure 4, was computed from the amplitude ratio and phase difference between the 2 Cartesian components of the electric field vector, both spatially averaged over the pupil plane (along the directions -u and w). Considering an aluminium coating for all mirrors and a reflection coefficient of 68% ( $\lambda=1 \mu\text{m}$ ) for the dichroic mirror  $M_9$ , the total transmission for a return path was 1.7%.

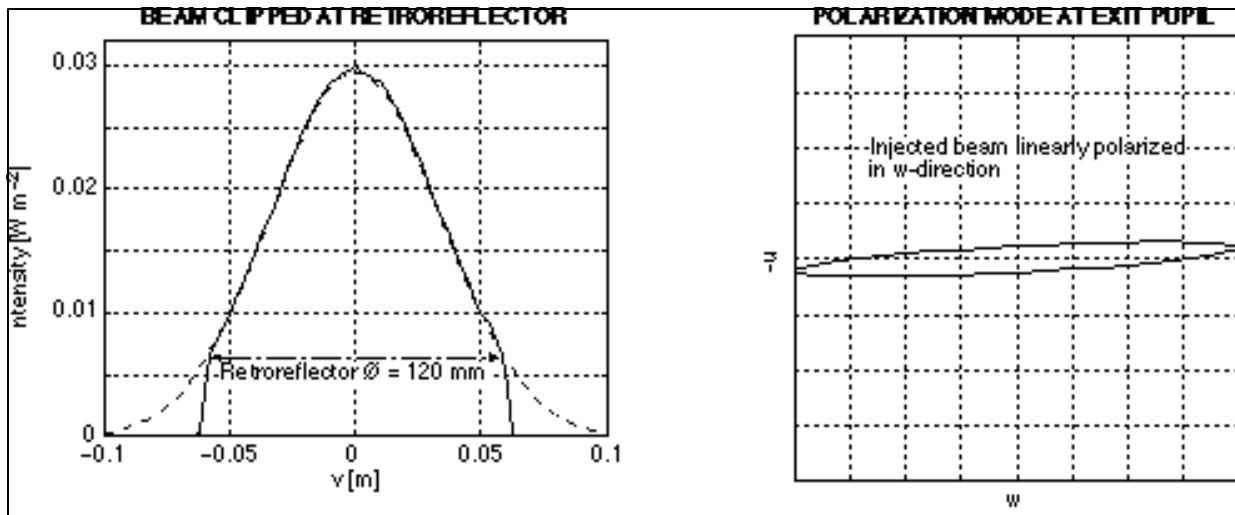


Figure 4: Beam intensity after Gaussian beam superposition (Left). Polarization state of retro-reflected beam (right)

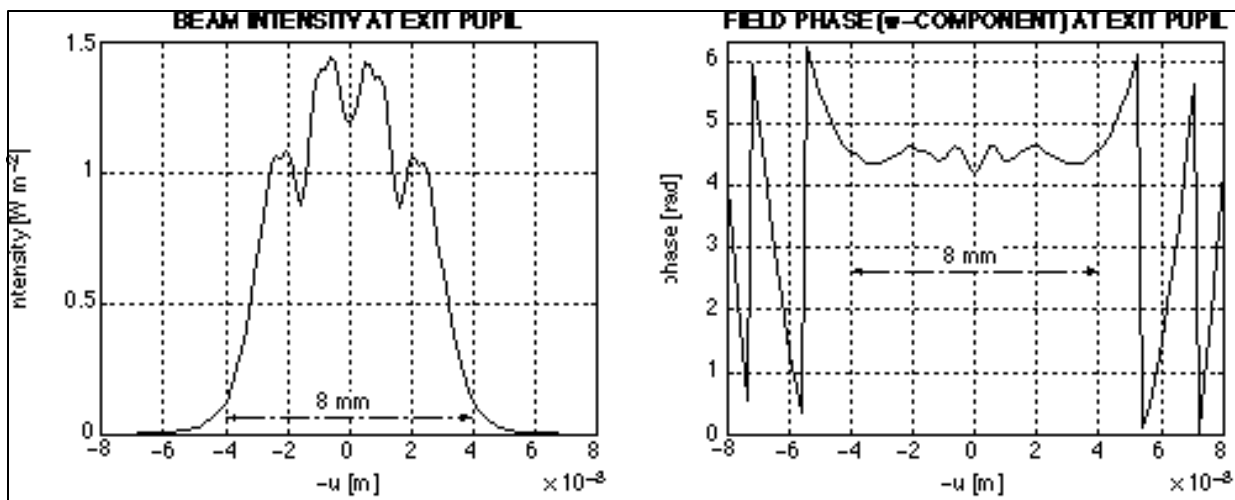


Figure 5: Intensity and phase profiles of the retro-reflected beam

The implementation of a polarized heterodyne interferometer using the central obscuration for the UT's appears feasible from a diffraction point of view. According to the simulation, the rotation of the polarisation state of the metrology beam is also acceptable. These results need to be confirmed by including the contribution of the retro-reflector to polarization rotation. A similar analysis is currently performed for the Auxiliary Telescopes, where the acceptable size of the retro-reflector is much smaller and the propagation path larger, both contributing to larger diffraction.

As a back-up solution, a non-polarized heterodyne scheme is foreseen<sup>5</sup>. However, this solution suffers from significant non-common path. In this framework, the implementation of integrated optics for both the metrology and the stellar beams could partially overtake this problem.

- **Metrology reference points**

In principle, the best location of the metrology reference points (also referred as retro-reflectors) is in a pupil plane. It is by definition the only location where any celestial field positions intersect. In this respect, the telescope secondary mirrors,  $M_2$ , would be the most attractive solution to host the metrology retro-reflector since it is the most "up-front" pupil position in the VLTI optical train. The image of the telescope central obscuration on  $M_2$  is respectively 155 mm for the UT's and 10.6 mm for the AT's, and interfaces already exist for mounting some light weight opto-mechanical devices.

The baseline for the retro-reflector is simply a lens collimating the laser beam on a corner cube. A holographic Optical Element (H.O.E) could be an elegant alternative to bulk optics. For PRIMA, its feasibility needs still to be demonstrated. It would have to comply with the following requirements:

- High efficiency to minimize the power losses of the metrology beam.
- High optical quality (compatible with an interferometry based internal metrology)
- Angle of acceptance of 430 arcsec (UT's) and 783.5 arcsec (AT's) for an hologram located on  $M_2$ .
- Depending on the details of the metrology system, the chromaticity and the impact on the Polarization state of the returned beam must be considered.

For a retro-reflector located at the center of the secondary mirror, the metrology beam will be reflected twice by the active mirror used for tilt correction (for the AT's and UT's) and the correction of higher order wavefront deformation (UT's only).

For "perfect" retro-reflector located at  $M_2$ , the tilt of the active mirror will not influence the direction of retro-reflected metrology beam. Only a slight lateral motion of this beam can occur in the delay line tunnel, after collimation by the Coudé relay optics. This affects the metrology beam monitoring the "off-axis" object  $S_2$ . This problem could be solved by making the Coudé focus "telecentric", as proposed in<sup>5</sup>, in the context of the PRIMA star separator.

In the case of the UT's, the atmospheric wavefront deformations corrected by the A.O deformable mirror ( $M_8$ ) for the stellar objects are unfortunately directly transferred to the metrology beams. For a retro-reflector covering the central obscuration on  $M_2$ , the diameter of the metrology beam, which is affected by the deformation of  $M_8$ , corresponds to the diameter of the central obscuration on  $M_8$ , i.e.  $\sim 14$ mm. A preliminary quantitative analysis has been performed using a "typical" phase map of the deformation of  $M_8$  generated to compensate a 0.66 arcsec seeing. Then, this phase map was used to simulate the metrology wavefront obtained after a double reflection on  $M_8$  and a "perfect" retro-reflection. Considering that a similar effect occurs in the second arm of the interferometer, Figure 6 shows the interference pattern corresponding to the superposition of the two metrology wavefronts. The area relevant for the metrology is the central obscuration represented by the black square box. In this case the visibility loss is about 20% for the central obscuration area.

In order to assess if the effect of the active mirror can be bypassed, the error on  $\Delta L$  was estimated when the path between  $M_2$  and the active mirror is not monitored by the metrology. Two field directions separated by 1 arcmin on the sky were considered and the corresponding sensitivity matrix of each mirror on  $\Delta L$  was computed using the VLTI end-to-end model<sup>8</sup>. For an angular perturbation of 20 arcsec and a translation perturbation of 20  $\mu\text{m}$  on each mirror, and considering uncorrelated errors between the telescopes, the variation of  $\Delta L$  reached about 40 nm for both UT's and AT's. This indicates that in the imaging mode of PRIMA the monitoring the optical path length between  $M_2$  and the active mirror could be avoided. However, in the astrometric mode (currently only foreseen with the AT's), the metrology must monitor the differential OPL as much "up-front" as possible.

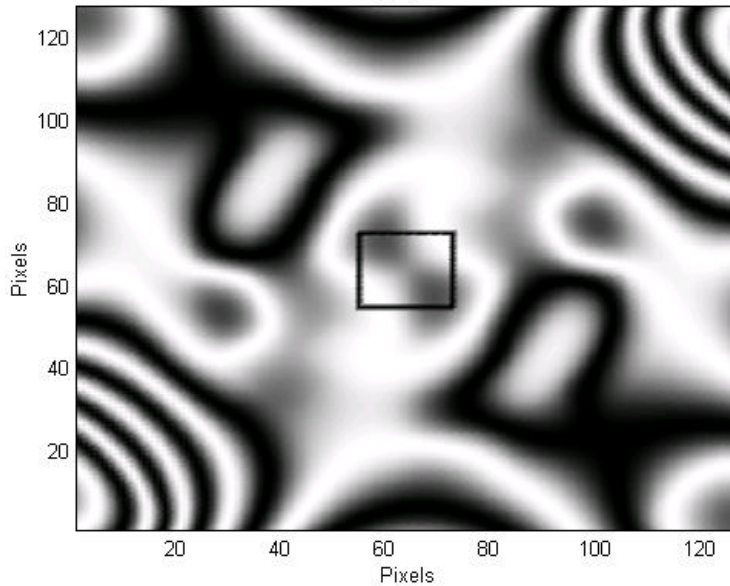


**Figure 6: Fringe pattern induced by a typical deformation of  $M_6$**

#### 4. IDENTIFICATION OF ERROR SOURCES

Table 1 lists the main sources of error of the metrology system according the following classification:

- **Layout errors**: these errors are due to non-common path (static or variable) between the metrology and the stellar beams and include misalignments. They translate the fact that one is trying to estimate an inappropriate quantity, although having a "perfect" sensor.
- **Instrumental errors**: They comprise the errors intrinsic to the sensor.

Errors related to the environmental conditions inside the VLTI (air dispersion/turbulence, thermal expansion of opto-mechanics...) are distributed among the above two types of errors. The list of identified error sources is the basis of the metrology system error budget currently under development. This error budget is used to specify the various sub-systems of the PRIMA metrology. As an example, Figure 7 shows the error resulting from detection noise, considering a given optical power and fringe visibility on the metrology detector. This analysis includes shot noise, thermal noise as well as residual laser intensity noise. It indicates that for a fringe visibility of 50%, the received power must reach about 500 nW to limit the optical path error to 1 nm.

<b>Error sources on DL</b>	
<b>Layout errors</b>	<b>Instrumental errors</b>
<ul style="list-style-type: none"> <li>• Beam routing (OPL offsets and misalignments) <i>Retro-reflector</i> <i>Beam injection/combination</i> <i>VLTI optical train</i> <i>Active mirror</i> <i>Air turbulence</i> <i>Mechanical stability</i> <i>Thermal effects</i></li> <li>• Wavefront distortion <i>Deformable mirror</i> <i>Internal air turbulence</i></li> <li>• Figuring errors associated with beam walk</li> <li>• Field dependent errors</li> </ul>	<ul style="list-style-type: none"> <li>• Laser head <i>Frequency stability</i> <i>Power stability</i></li> <li>• Electronics <i>Detection noise (V,P,SNR)</i> <i>Signal conditioning noise</i> <i>Demodulation noise</i></li> <li>• Optical cross-talk</li> <li>• Metrology Wavelength dependent errors <i>Chromatic errors on coatings</i> <i>Air dispersion</i></li> <li>• Drift of "zero" point (dead path)</li> </ul>

**Table 1: Main error sources of the metrology system**



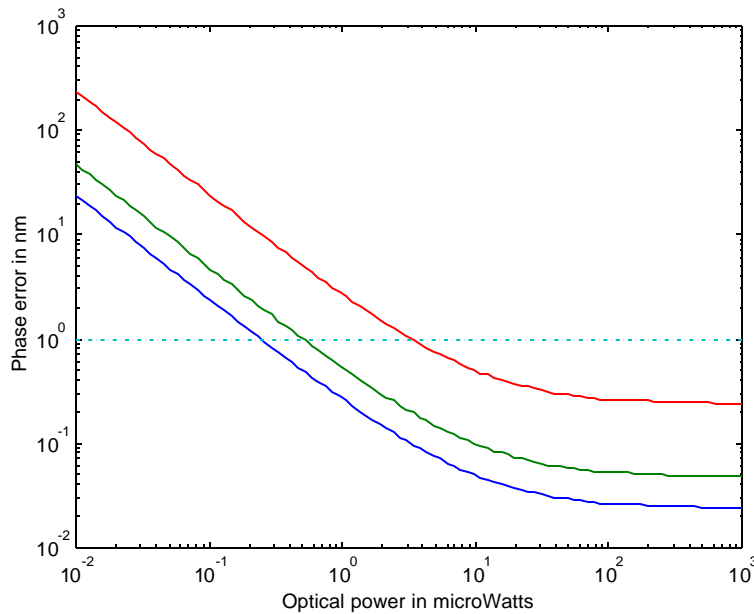


**Figure 7: Electronics induced phase error ( $l=1$  mm) as a function of the detected optical power. Three fringe visibilities were considered: lower curve,  $V=1$ ; middle curve  $V=0.5$ ; top curve  $V=0.1$ ;**

## 5. CONCLUSION

The PRIMA metrology system must clearly meet an ambitious accuracy goal. A baseline for this metrology system has been identified, including a phase demodulation architecture. The next steps will include the consolidation of the metrology error budget. The development of a prototype of the phase meter is planned in the course of this year and measurements will be performed at Paranal to characterize in more detail the effect of internal turbulence in the context of PRIMA.

## 6. ACKNOWLEDGMENTS

The author would like to thank U.Johann, E.Manske, R.Sesselmann from Dornier Satellitensystem GmbH for fruitful discussion about the metrology system during the PRIMA feasibility Study, as well as Y.Salvadé, A.Courteville, and R.Dändliker from the Institute of Micro-Technology in Neuchâtel, who conducted the PRIMA metrology rider study. The contribution of R.Wilhelm, who simulated the gaussian beam propagation, is gratefully acknowledged.

## 7. REFERENCES

1. F. Delplancke et al. "Phase-referenced imaging and micro-arcsecond astrometry with the VLTI", these proceedings.
2. L. D'Arcio, "Selected aspects of wide-field stellar interferometry", Ph.D. Thesis, University of Delft, Nov. 1999, ISBN 90-6464-016-6.
3. Ph.Gitton, B.Koehler, S.Lévêque, A.Glindemann, "The VLT Interferometer-Preparation for first fringes", these proceedings.
4. O.von der Luehe, A.Quirrenbach, B.Koehler, "Narrow Angle Astrometry with the VLT Interferometer", in Science with the VLTI, ESO Astrophysics symposia, editors J.R.Walsh and I.J.Danziger, ISBN 3-540-59169-9, 1995
5. U.Johann et al, "Prima Feasibility Study", Dornier Satellitensysteme GmbH, ESO technical report VLT-TRE-DSS-15700-0001, July 1999.
6. Y.Salvadé, A.Courteville, R.Dändliker, "PRIMA metrology rider study", Institute of Micro-Technology of Neuchâtel, ESO technical report VLT-TRE-IMT-15700-0001, January 2000.
7. Y.Salvadé, A.Courteville, R.Dändliker, "Absolute metrology for the Very Large Telescope Interferometer", these proceedings.
8. R. Wilhelm, B. Koehler, "Modular toolbox for dynamic simulation of astronomical telescopes and its application to the VLTI", these proceedings